ACADEMIC PRESS

Journal of Solid State Chemistry 169 (2002) 125–130

JOURNAL OF SOLID STATE CHEMISTRY

www.academicpress.com

Magnetic and calorimetric studies on ordered perovskite Ba_2ErRuO_6

Yuki Izumiyama,[a] Yoshihiro Doi,[a] Makoto Wakeshima,[a] Yukio Hinatsu,[a,*] Akio Nakamura,[b] and Yoshinobu Ishii[b]

[a] *Division of Chemistry, Graduate School of Science, Hokkaido University, Sapporo 060-0810, Japan*
[b] *Japan Atomic Energy Research Institute, Tokai-mura, Ibaraki 319-1195, Japan*

Received 23 April 2002; received in revised form 3 September 2002; accepted 12 September 2002

Abstract

Magnetic properties of an ordered perovskite compound Ba_2ErRuO_6 have been reported. We have performed powder neutron diffraction measurements at 10 K and room temperature to investigate its crystal and magnetic structures. As a result of the refinement of the data collected at room temperature, it has been found that the crystal structure of this compound is a cubic perovskite ($a = 8.323(1)$Å) with the space group $Fm\bar{3}m$ and the 1:1 ordered arrangement of Er^{3+} and Ru^{5+} over the six-coordinate *B* sites. From the magnetic susceptibility and specific heat measurements, this compound shows two magnetic anomalies at 10 and 40 K. The analysis of the temperature dependence of the magnetic specific heat indicates that the anomaly at 40 K is due to the antiferromagnetic ordering of Ru^{5+} ions and the anomaly at 10 K is ascribable to the magnetic interactions between Er^{3+} ions. Neutron diffraction data collected at 10 K show that the Ba_2ErRuO_6 has a long-range ferromagnetic ordering involving both Er^{3+} and Ru^{5+}. Each of their magnetic moments orders in a Type I arrangement and these magnetic moments are antiparallel in the *ab*-plane with each other.

Keywords: Magnetic properties; Specific heat; Perovskite; Magnetic structure; Ruthenium; Erbium

1. Introduction

In recent years, the solid-state chemistry of mixed-metal oxides containing platinum group metals has attracted a great deal of interest. These materials adopt a diverse range of structures and show a wide range of electronic properties [1–4]. We have focused our attention on the structural chemistry and magnetic properties of ordered perovskite-type oxides A_2LnMO_6 (A = Sr, Ba; Ln = lanthanide elements; $M = 4d$ or $5d$ transition elements), in which the Ln and M ions regularly order [5–10]. These oxides show a variety of magnetic behavior at low temperatures. We are particularly interested in such compounds containing pentavalent ruthenium ions. The electronic structure of Ru^{5+} is [Kr]$4d^3$ ([Kr]: krypton electronic core). Such highly oxidized cations from the second transition series sometimes show quite unusual magnetic properties. Most of the A_2LnRuO_6 compounds show antiferromagnetic transitions at 15–30 K [10–13].

Now, we have paid attention to a compound Ba_2ErRuO_6 in which both the erbium and ruthenium ions are accommodated at the *B* sites of the perovskite ABO_3 and they both contribute to the magnetic properties of this compound. Previously, Battle et al. investigated the crystal structure of Sr_2ErRuO_6 and found that the structure is that of a distorted perovskite with a 1:1 ordered arrangement of Er^{3+} and Ru^{5+} over the six-coordinate sites [5,13]. Its magnetic susceptibility measurements showed magnetic anomalies at 40 and 10 K. Neutron diffraction data collected at 4.2 K showed the presence of long-range antiferromagnetic order involving both Er^{3+} and Ru^{5+} [13]. This compound orders as a Type I antiferromagnet. This magnetic structure is envisaged in a pseudo-cubic unit cell of size $\sim 2a_p \times 2a_p \times 2a_p$ (a_p: the primitive perovskite unit cell), such that both the Er^{3+} and Ru^{5+} ions form two interpenetrating face-centered sublattices. The directions of magnetic moments are parallel to the *a*-axis.

*Corresponding author. Fax: +81-11-706-2702.
E-mail address: hinatsu@sci.hokudai.ac.jp (Y. Hinatsu).

0022-4596/02/$ - see front matter © 2002 Elsevier Science (USA). All rights reserved.
PII: S0022-4596(02)00041-5

When the barium ion is situated at the A site of the perovskite ABO_3, the deviation from the cubic symmetry of the BO_6 octahedral coordination is expected to be much smaller than the case for A = Sr. In this paper, we will report the crystal and magnetic structures and the magnetic properties of Ba_2ErRuO_6 through measurements of its magnetic susceptibility, specific heat and powder neutron diffraction. In addition, we have determined the electronic state of the Er^{3+} ion in the Ba_2ErRuO_6 from the analysis of the temperature dependence of its magnetic entropy data.

2. Experimental

A polycrystalline sample of Ba_2ErRuO_6 was prepared by firing the appropriate amounts of $BaCO_3$, Er_2O_3 and RuO_2, first at 900°C for 12 h and then 1200°C for 60 h in air with several interval regular grinding and pelleting. A diamagnetic Ba_2LuNbO_6 was also prepared. This compound is isomorphous with Ba_2ErRuO_6 and is needed to estimate the lattice contribution of the specific heat to the total specific heat of Ba_2ErRuO_6. As starting materials, $BaCO_3$, Lu_2O_3 and Nb_2O_5 were used. In addition, a couple of compounds Ba_2YRuO_6 and Ba_2YNbO_6 were also prepared by firing the appropriate amounts of $BaCO_3$, Y_2O_3, RuO_2 and Nb_2O_5. These two compounds are needed to estimate the magnetic entropy due to the magnetic ordering of Ru^{5+} ions, as will be described later. The heating procedures were the same as the case for Ba_2ErRuO_6. The progress of the reactions was monitored by powder X-ray diffraction measurements.

Powder X-ray diffraction measurements were carried out in the region of $10^\circ \leqslant 2\theta \leqslant 120^\circ$ using Cu$K\alpha$ radiation on a Rigaku MultiFlex diffractometer equipped with a curved graphite monochromator.

Powder neutron diffraction profiles were measured at 10 K and room temperature using a high-resolution powder diffractometer at the JRR-3M reactor (Japan Atomic Energy Research Institute), with a Ge (331) monochromator ($\lambda = 1.8230$ Å) [14]. The collimators used were 6′–20′–6′, which were placed before and after the monochromator, and between the sample and each detector. The set of 64 detectors and collimators, which were placed at intervals of 2.5° rotate around the sample. Measurements were performed in the range of $10^\circ \leqslant 2\theta \leqslant 120^\circ$. Crystal and magnetic structures were determined by the Rietveld technique, using program RIETAN [15].

The temperature dependence of the magnetic susceptibility was made in an applied field of 0.1 T over the temperature range $1.8\,K < T < 300\,K$, using a SQUID magnetometer (Quantum Design, MPMS5S). The susceptibility measurements were performed either using zero-field cooling (ZFC) and field cooling (FC) conditions. The former was measured upon heating the sample to 300 K under the applied magnetic field of 0.1 T after zero-field cooling to 1.8 K. The latter was measured upon cooling the sample from 300 to 1.8 K at 0.1 T.

Specific heat measurements were performed using a relaxation technique by a commercial heat capacity measuring system (Quantum Design, PPMS) in the temperature range 1.8–300 K. The sintered sample in the form of a pellet was mounted on a thin alumina plate with Apiezon for better thermal contact.

3. Results and discussion

3.1. Crystal structure

The X-ray diffraction data collected on Ba_2ErRuO_6 could be indexed in a cubic unit cell with $a = 8.323(1)$ Å and space group $Fm\bar{3}m$. Its crystal structure is illustrated in Fig. 1. The deviation from the cubic symmetry of the BO_6 octahedral coordination is not observed in this compound, which is contrastive to the structure of Sr_2ErRuO_6 [5,13]. Most of a series of Ba_2LnRuO_6 (Ln = La, Pr, Nd, Eu) are monoclinic with space group $P2_1/n$ [11,12,16–17], but two compounds Ba_2YRuO_6 and Ba_2LuRuO_6 adopt the same cubic perovskite structure with the case for Ba_2ErRuO_6 [18]. This space group $Fm\bar{3}m$ also allows two crystallographically distinct octahedral sites in the double perovskite structure, thus permitting 1:1 ordered arrangement between Ru^{5+} and Er^{3+} ions.

Since the neutron diffraction measurements were carried out at room temperature, we have performed the Rietveld analysis for the neutron diffraction data using a program RIETAN [15]. Fig. 2(a) shows the

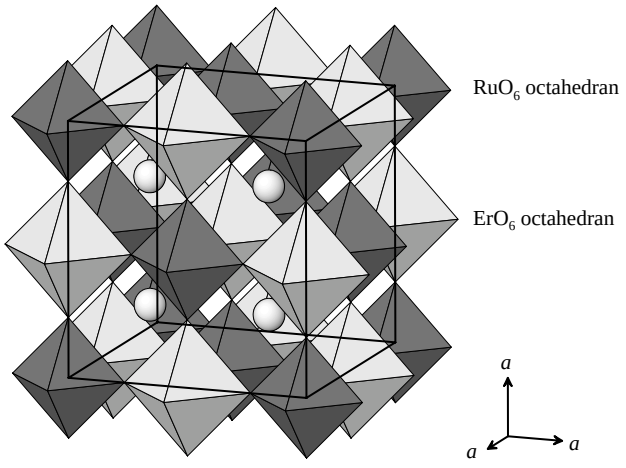

Fig. 1. The crystal structure of Ba_2ErRuO_6. The solid lines indicate the cubic unit cell.

calculated and observed diffraction profiles at room temperature.

Lattice parameters and atomic positions which are refined by using the neutron diffraction data are tabulated in Table 1. The Ru–O bond length (1.954 Å) is almost equal to those in various Ru^{5+} compounds [10–12,16–18] and is shorter than those in Ru^{4+} compounds, for example in $BaRuO_3$ [19]. This result also supports that ruthenium ions in the Ba_2ErRuO_6 are in the pentavalent state.

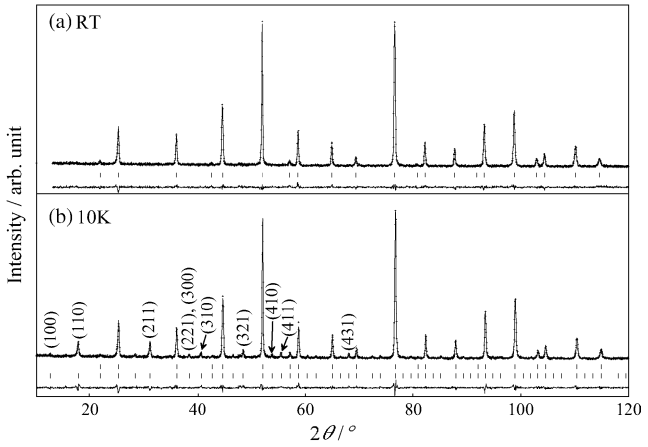

Fig. 2. Powder neutron diffraction profiles for Ba_2ErRuO_6 at room temperature (a) and 10 K (b). The calculated and observed profiles are shown on the top solid line and cross markers, respectively. For (a), the vertical marks in the middle show positions calculated for Bragg reflections. For (b), the nuclear reflection positions are shown as upper vertical marks and magnetic ones are shown as lower ones. The lower trace is a plot of the difference between calculated and observed intensities.

3.2. Magnetic properties

The temperature dependence of the magnetic susceptibilities for Ba_2ErRuO_6 is shown in Fig. 3(a). It is found that a magnetic anomaly has been found at 10 K. In addition, another small magnetic anomaly has been observed at 40 K. This anomaly is not clear in the magnetic susceptibility vs temperature curve, the reason for which will be described later. No divergence has been observed between the ZFC and FC magnetic susceptibilities in the whole temperature range for this cubic Ba_2ErRuO_6. From the magnetic susceptibility measurements, Sr_2ErRuO_6 also shows two magnetic anomaly at 10 and 40 K and very clear divergence between the ZFC and FC magnetic susceptibilities has been observed below the magnetic transition temperatures [5]. These experimental results indicate that the monoclinic Sr_2ErRuO_6 [5,13] is not an ideal antiferromagnet. We consider that this is due to the contribution of the weak ferromagnetic component to its magnetic properties [5]. In the case of the compound with a low crystal symmetry such as monoclinic symmetry, the Dzyaloshinsky–Moriya interaction can exist between the ordered magnetic moments, which results in the existence of a weak ferromagnetic component in the susceptibilities. Fig. 3(b) shows the variation of the reciprocal susceptibility against temperature. In the paramagnetic region ($T > 40$ K), the fitting of the Curie–Weiss law to the temperature dependence of magnetic susceptibilities gives the effective magnetic moment (μ_{eff}) and Weiss constant (θ) to be 9.52(2) μ_B and −14.6(5) K, respectively. Since the theoretical magnetic moments of Ru^{5+} and Er^{3+} (free ion) are 3.87 and 9.57 μ_B, respectively, the expected effective magnetic

Table 1
Structural parameters for Ba_2ErRuO_6

Atom	Site	x	y	z	B (Å^2)	m (μ_B)
At room temperature, space group $Fm\bar{3}m$						
Ba	8*c*	1/4	1/4	1/4	0.36(4)	
Er	4*b*	1/2	1/2	1/2	0.33(6)	
Ru	4*a*	0	0	0	0.14(7)	
O	24*e*	0.2348(2)	0	0	0.70(4)	
$a = 8.323(1)$ Å	$V = 576.6(2)$ Å^3					
$R_{WP} = 10.45\%$	$R_I = 2.95\%$					
At 10 K, space group $Fm\bar{3}m$						
Ba	8*c*	1/4	1/4	1/4	0.16(6)	
Er	4*b*	1/2	1/2	1/2	0.58(8)	4.43(8)
Ru	4*a*	0	0	0	0.10(10)	2.87(13)
O	24*e*	0.2351(2)	0	0	0.62(5)	
$a = 8.298(1)$ Å	$V = 571.4(1)$ Å^3					
$R_{WP} = 10.92\%$	$R_I = 2.61\%$, $R_I(\text{mag}) = 9.18\%$					

Note: Definition of reliability factors R_{WP} and R_I are given as follows:

$$R_{WP} = \left[\sum w(|F(o)| - |F(c)|)^2 / \sum w|F(o)|^2\right]^{1/2}, \quad R_I = \sum |I_k(o) - I_k(c)| / \sum I_k(o).$$

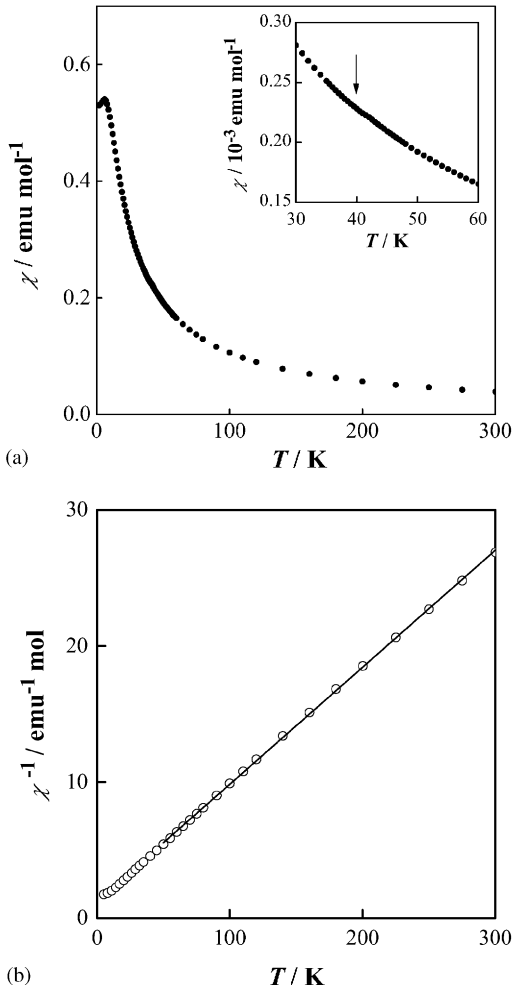

Fig. 3. (a) Temperature dependence of the magnetic susceptibilities for Ba_2ErRuO_6. No divergence has been observed between the ZFC and FC magnetic susceptibilities in the whole temperature range. A vertical arrow in the inset shows a magnetic anomaly at 40 K (see text). (b) The reciprocal magnetic susceptibilities against temperature. A solid line shows the Curie–Weiss fitting.

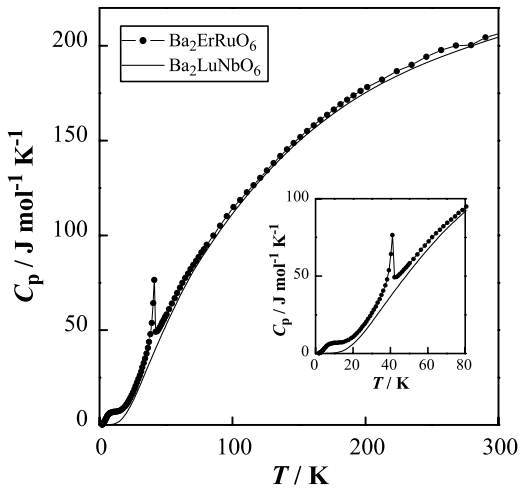

Fig. 4. Temperature dependence of the specific heat for Ba_2ErRuO_6 and Ba_2LuNbO_6.

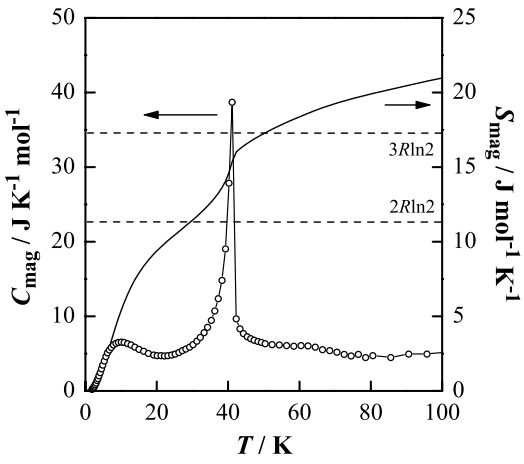

Fig. 5. The magnetic specific heat (C_{mag}) and magnetic entropy (S_{mag}) against temperature for Ba_2ErRuO_6.

moment ($\sim 10.3\,\mu_B$) is estimated from the relation $\mu_{eff} = \sqrt{\mu^2_{Ru^{5+}} + \mu^2_{Er^{3+}}}$. The value obtained from the experiment is lower than the calculated value. This result may suggest that the magnetic ions in this compound are affected by the crystal field to some extent. The negative Weiss constant indicates that the predominant magnetic interaction in Ba_2ErRuO_6 is antiferromagnetic.

Fig. 4 shows the variation of the specific heat for Ba_2ErRuO_6 as a function of temperature. The results of the specific heat measurements are consistent with those by the magnetic susceptibility measurements (Fig. 3(a)), i.e., a λ-type specific heat anomaly has been observed at 40 K, and another anomaly has been found at ca. 10 K.

In the same figure, Fig. 4, the specific heat data for Ba_2LuNbO_6 (which is isomorphous with Ba_2ErRuO_6) are also plotted. This Ba_2LuNbO_6 is diamagnetic, i.e., it has no magnetic ions. If we assume that the electronic and lattice contribution to the specific heat are equal between Ba_2ErRuO_6 and Ba_2LuNbO_6, the magnetic specific heat (C_{mag}) for Ba_2ErRuO_6 is obtained by subtracting the specific heat of Ba_2LuNbO_6 from that of Ba_2ErRuO_6. The temperature dependence of the magnetic specific heat (C_{mag}) and the magnetic entropy (S_{mag}) is shown in Fig. 5. The magnetic entropy change associated with the antiferromagnetic transition is obtained to be $\sim 18\,J\,mol^{-1}K^{-1}$ (at 60 K) by integrating $S_{mag}(T) = \int (C_{mag}/T)dT$. This magnetic entropy is near to $3R(2S+1) = 3R\ln(2\times\frac{1}{2}+1) = 3R\ln 2 = 17.3\,J\,mol^{-1}\,K^{-1}$ where R is a molar gas constant and S is a total spin quantum number. Present measurements of the temperature dependence of the magnetic susceptibility and specific heat indicate that there exist two magnetic transitions. We consider that the transition observed at ca. 10 K is due to the magnetic interactions between Er^{3+} ions and the transition

observed at 40 K is ascribable to the antiferromagnetic orderings of Ru^{5+} ions. The reason why the magnetic transition at 40 K is not clear in the magnetic susceptibility vs temperature curve is due to the smaller magnetic moment of the Ru^{5+} ion (3.87 μ_B) compared with that of the Er^{3+} ion (9.57 μ_B).

To estimate the magnetic entropy change for the magnetic ordering of Ru^{5+} ions, we evaluated it from the specific heat measurements on Ba_2LnRuO_6 (Ln = Y, Lu) in which only the Ru^{5+} ions are paramagnetic. Both the compounds show an antiferromagnetic transition at 37 K which is due to the magnetic interactions between Ru^{5+} ions [16,17]. Fig. 6(a) shows the temperature dependence of the magnetic susceptibility and the specific heat for Ba_2YRuO_6. The magnetic entropy change due to the magnetic ordering of Ru^{5+} ions at 37 K was determined by assuming that the electronic and lattice contribution to the specific heat of the Ba_2YRuO_6 was equal to the specific heat of a diamagnetic Ba_2YNbO_6. Fig. 6(b) shows the temperature dependence of the magnetic specific heat and the magnetic entropy for Ba_2YRuO_6. The magnetic entropy is 3.9 J mol^{-1} K^{-1}, which is close to $R\ln(2S+1) = R\ln(2\times\frac{1}{2}+1) = 5.76$ J mol^{-1} K^{-1}. This result means

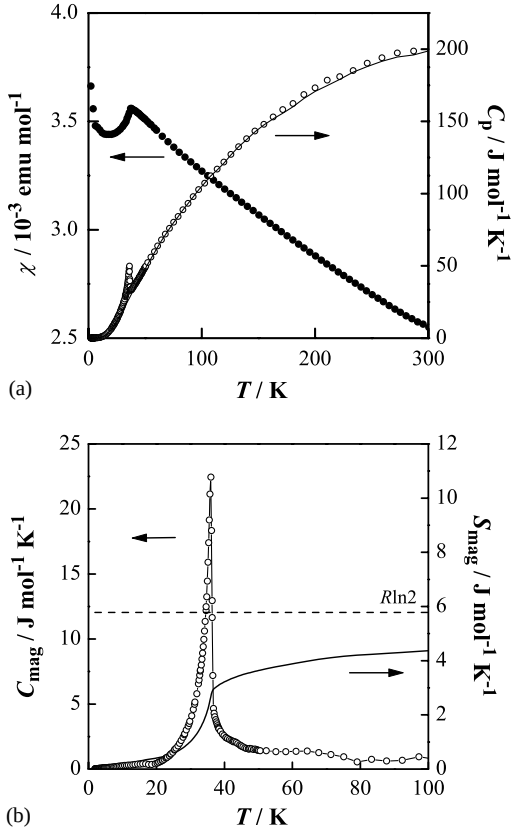

Fig. 6. (a) Temperature dependence of the magnetic susceptibility (●) and specific heat (○) for Ba_2YRuO_6. A solid line represents the specific heat for Ba_2YNbO_6 (see text). (b) The magnetic specific heat (C_{mag}) and magnetic entropy (S_{mag}) against temperature for Ba_2YRuO_6.

that the ground state of the Ru^{5+} ion should be a doublet. That is, although a total spin quantum number of the Ru^{5+} ion is calculated to be $S=\frac{3}{2}$, the four degenerating states split into two doublets $|S=\frac{3}{2}, M_S=\pm\frac{3}{2}\rangle$, and $|S=\frac{3}{2}, M_S=\pm\frac{1}{2}\rangle$ [20]. When the same estimation for the magnetic entropy change of Ru^{5+} ions holds for the case of Ba_2ErRuO_6, the rest of the magnetic entropy due to the magnetic ordering of Er^{3+} ions is $3R\ln 2 - R\ln 2 = 2R\ln 2 = R\ln 4$. This result indicates that the degeneracy of the ground state of Er^{3+} ion should be four, because the magnetic entropy is given by $R\ln W$ (W: degeneracy). In the Ba_2ErRuO_6, where the Er^{3+} ions are surrounded by six-coordinated oxygen ions, the ground state multiplet $^4I_{15/2}$ of the Er^{3+} ion splits and a Γ_7 doublet or a Γ_8 quartet becomes a ground state in the octahedral crystalline electric field [21]. The results of the specific heat measurements suggest that the ground state of the Er^{3+} ion should be the Γ_8 quartet. The variation of the magnetic entropy with temperature (Fig. 5) implies that the ordering of the magnetic moments of Er^{3+} ions gradually occurs when the temperature is decreased through 30 K.

3.3. Magnetic structure

The neutron diffraction data collected at 10 K are depicted in Fig. 2(b). A number of low-angle peaks which were not observed at room temperature appear, indicating that Ba_2ErRuO_6 exhibits long-range magnetic ordering at this temperature. At 10 K, this Ba_2ErRuO_6 has the same crystal structure as that at room temperature. In the analysis of the neutron diffraction data measured at 10 K, we assumed that all the magnetic moments were collinear since no magnetic satellite reflections exist. In addition, the size of the magnetic unit cell is as large as that of the crystal unit cell, since there appeared no superlattice reflections, and thus the magnetic unit cell is described as $2a_p \times 2a_p \times 2a_p$, where a_p means a lattice parameter in a primitive cubic perovskite unit cell. In this unit cell, the Er^{3+} and Ru^{5+} ions form two interpenetrating face-centered sublattices. Then, we have performed the Rietveld analysis and succeeded in determining the magnetic structure, which is illustrated in Fig. 7. In this magnetic structure, each of the magnetic moments of Er^{3+} and Ru^{5+} orders in a Type I arrangement. The magnetic moments of the Er^{3+} and Ru^{5+} ions which exist on the *ab*-plane are ordered antiferromagnetically, and the *ab*-planes would be ferrimagnetic planes. After all, Ba_2ErRuO_6 is an antiferromagnet in which the ferrimagnetic *ab*-planes are stacked antiferromagnetically along the *c*-axis. This magnetic structure is almost the same as that for Sr_2ErRuO_6 [13]. The ordered magnetic moments are determined to be 4.43(8) μ_B for Er^{3+} and 2.87(13) μ_B for Ru^{5+}. Since the theoretical value of the

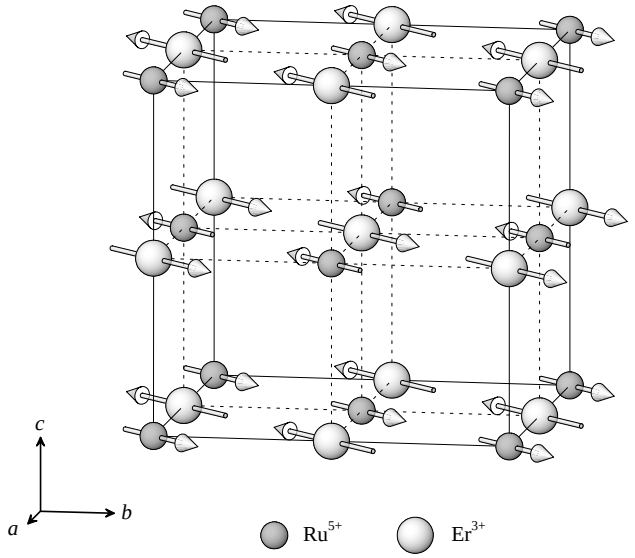

Fig. 7. The magnetic structure of Ba_2ErRuO_6. Diamagnetic ions are omitted. Larger circles Er^{3+}; smaller circles Ru^{5+}. Arrows show the direction of the magnetic moments.

magnetic moment for the Ru^{5+} ion which has a d^3 electronic configuration is 3.0 μ_B, it can be said that the magnetic moment of the Ru^{5+} ion in Ba_2ErRuO_6 is almost saturated at 10 K. The results of the magnetic susceptibility, specific heat and magnetic entropy measurements for Ba_2ErRuO_6 demonstrate that the magnetic order of the Ru^{5+} ions occurs at 40 K, and accordingly it is valid that the ordered magnetic moments of the Ru^{5+} ions are saturated at 10 K. On the other hand, the magnetic moment of the Er^{3+} ion which is estimated to be 4.43(8) μ_B from the analysis of the neutron diffraction data is approximately half the theoretical value for the free Er^{3+} ion, 9.0 μ_B. One reason for this is that this experimental temperature (10 K) is too high to determine the ordered magnetic moment of Er^{3+} ion. Similar small ordered moments of the Er^{3+} ions have been reported for the Sr_2ErRuO_6 (4.0 μ_B at 10 K and 4.7 μ_B at 4.2 K) [13]. This result also indicates that we should consider the crystal field effect on the magnetic moments of the Er^{3+} ions.

References

[1] A. Callaghan, C.W. Moeller, R. Ward, Inorg. Chem. 5 (1966) 1572–1576.
[2] Y. Maeno, H. Hashimoto, K. Yoshida, S. Nishizaki, T. Fujita, J.G. Bednorz, F. Lichtenberg, Nature 372 (1994) 532–534.
[3] N. Taira, M. Wakeshima, Y. Hinatsu, J. Solid State Chem. 144 (1999) 216–219.
[4] C. Bernhard, J.L. Tallon, Ch. Niedermayer, Th. Blasius, A. Golnik, E. Brucher, R.K. Kremer, D.R. Noakes, C.E. Stronach, E.J. Ansaldo, Phys. Rev. B 59 (1999) 14099–14107.
[5] Y. Doi, Y. Hinatsu, J. Phys.: Condens. Matter 11 (1999) 4813–4820.
[6] D. Harada, M. Wakeshima, Y. Hinatsu, J. Solid State Chem. 145 (1999) 356–360.
[7] K. Henmi, Y. Hinatsu, N. Masaki, J. Solid State Chem. 148 (1999) 353–360.
[8] M. Wakeshima, D. Harada, Y. Hinatsu, J. Mater. Chem. 10 (2000) 419–422.
[9] D. Harada, M. Wakeshima, Y. Hinatsu, K. Ohoyama, Y. Yamaguchi, J. Phys.: Condens. Matter 12 (2000) 3229–3239.
[10] Y. Doi, Y. Hinatsu, K. Oikawa, Y. Shimojo, Y. Morii, J. Mater. Chem. 10 (2000) 797–800.
[11] Y. Izumiyama, Y. Doi, M. Wakeshima, Y. Hinatsu, K. Oikawa, Y. Shimojo, Y. Morii, J. Mater. Chem. 10 (2000) 2364–2367.
[12] Y. Izumiyama, Y. Doi, M. Wakeshima, Y. Hinatsu, K. Oikawa, Y. Shimojo, Y. Morii, J. Phys.: Condens. Matter 13 (2001) 1303–1313.
[13] P.D. Battle, C.W. Jones, F. Studer, J. Solid State Chem. 90 (1991) 302–312.
[14] Y. Morii, J. Cryst. Soc. Jpn. 34 (1992) 62.
[15] F. Izumi, in: R. A.Young (Ed.), The Rietveld Method, Oxford University Press, Oxford, 1993 (Chapter 13).
[16] P.D. Battle, J.B. Goodenough, R. Price, J. Solid State Chem. 46 (1983) 234–244.
[17] P.D. Battle, W.J. Macklin, J. Solid State Chem. 54 (1984) 245–250.
[18] P.D. Battle, C.W. Jones, J. Solid State Chem. 78 (1989) 108–116.
[19] A. Santoro, I. Natali Sora, Q. Huang, J. Solid State Chem. 151 (2000) 245–252.
[20] D. Harada, Y. Hinatsu, J. Solid State Chem. 158 (2001) 245–253.
[21] K.R. Lea, M.J.M. Leask, W.P. Wolf, J. Phys. Chem. Solids 23 (1962) 1381–1405.